

# Study of failure of EB-PVD thermal barrier coating upon near- $\alpha$ titanium alloy

Bo He · Fei Li · Hong Zhou · Yongbing Dai ·  
Baode Sun

Received: 29 November 2006 / Accepted: 3 October 2007 / Published online: 31 October 2007  
© Springer Science+Business Media, LLC 2007

**Abstract** The cracking failure of a conventional thermal barrier coating (TBC), consisting of a near- $\alpha$  titanium substrate, a NiCoCrAlY bond coat (BC), and a 8 wt.% yttria-stabilized zirconia ceramic layer deposited by electron beam-physical vapor deposition (EB-PVD) method, was studied by cyclic furnace testing and isothermal exposure. The scanning electron microscope, electron probe microanalysis, and microhardness indentation were used to probe the failure mechanism. It is found that due to the mismatch of the coefficient of thermal expansion, the as-deposited BC is suffered the long-term tensile creeping at room temperature. During the high-temperature exposure, the TBC locally rumples, bringing in-plane tensile stress at the shoulders, and out-of-plane tensile stress at the peak of the ruffled BC, where primal cracks are originated. During the cooling period, the ridges of substrate pulled by the local rumpling of the BC blocks the contracting of the BC, originating new cracks in planar BC, and aggravating the original cracks. Furthermore, the oxidation products pushed into the BC and the 8YSZ enlarges the TBC and cracks the substrate along the weakest diffused grain boundaries. The cracking failure related to the diffusion of the BC to the substrate is also discussed.

## Introduction

The titanium alloys, on account of their excellent specific strength and acceptable thermal tolerance, have been

widely applied in elevated temperature environments. However, their highest service temperature is strictly limited under 600 °C because of the oxidation and embrittlement [1, 2]. Many efforts have been dedicated so far to develop the oxidation-resistance of the titanium alloys by kinds of coatings [3–8]. However, most of them do not pay enough attentions on the heat-resistance of the coatings, so inevitably, some mechanical properties of the titanium alloy substrate will be degraded in high-temperature environment [7, 9, 10]. Therefore, both oxidation- and heat-resistance should be taken into considering simultaneously in improving the high-temperature performance of the titanium alloys. For this purpose, the applying of the thermal barrier coatings (TBCs) on titanium alloys may be worthy to be considered.

Conventional duplex thermal barrier coating comprising of an oxidation-resistant bond coating (BC) and a top heat-resistant ceramic layer has been regarded as an effective surface thermal isolating technology for the increase of component durability for decades [11]. Generally, the ceramic layer is 8 wt.% yttria-stabilized zirconia (8YSZ) and the BC is NiCoCrAlY intermetallics. Figure 1 shows the schematically layers of a conventional TBC. Among all layers of a TBC system, the bond coat is essentially important because it is deeply related with both the endurance and the performance of a TBC [11], so the chemical and physical properties of the BC and the substrate should be similar each other. Thus, to apply a Ni-based BC to a Ti-based substrate will unavoidably be confronted with the compatibility problem. However, since the 8YSZ/NiCoCrAlY duplex TBC is a mature and practical TBC so far, and the knowledge about it can also be used as references in current study. Besides, it is still scarce in detail in applying of the 8YSZ/NiCoCrAlY duplex TBC to the titanium alloys and the study to the failure process

B. He · F. Li · H. Zhou · Y. Dai · B. Sun (✉)  
State Key Laboratory of Metal Matrix Composites, School of  
Materials Science and Engineering, Shanghai Jiao Tong  
University, 800, Dongchuan Road, Shanghai 200240, PR China  
e-mail: bdsun@sjtu.edu.cn

and mechanism. So, current work will absolutely help the further study for improving the high-temperature performance of the titanium alloys.

In this article, a conventional duplex NiCoCrAlY/8YSZ TBC was deposited on a near- $\alpha$  Ti-based substrate by EB-PVD method, the failure mechanism of TBC is described in detail by the thermal cycling test, isothermal exposure, and metallographic observations.

## Experimental procedure

### Materials

The starting materials for the preparation of BC and top ceramic coating were Ni-23.7Co-20.34Cr-8.56Al-0.91Y (in wt.%) and 8 wt.%Y<sub>2</sub>O<sub>3</sub>-ZrO<sub>2</sub> (in wt.%), respectively. The near- $\alpha$  titanium alloy substrates were cut from a wrought TC11 (Ti-6.5Al-3.3Mo-1.8Zr-0.26Si, in wt.%) ingot into disks with the dimensions of  $\varnothing 20$  mm  $\times$  8 mm.

In order to obtain better bonding quality, the substrates were firstly polished with 1200# fine emery paper and subsequent diamond slurries from 5 to 1  $\mu$ m. After super-sonic cleaned in anhydrous alcohol and air dried, the BC and the YSZ were deposited in sequence by EB-PVD on both planar surfaces of the substrates to the thickness of  $\sim 50$  and  $\sim 100$   $\mu$ m, respectively. During deposition, the substrates were clamped and rotated above the vapor source in order to obtain uniform thickness and properties. Figure 1 shows the cross-section of as-deposited sample and its schematic illustration of layered structure.

### Thermal cycling

The service temperature of TBC-protected near- $\alpha$  titanium alloy is desired  $\sim 200$  °C higher than that of the uncoated ones [11], so the thermal cycling test was conducted at 800 °C under atmospheric pressure in static air for evaluation the durability of the TBC. The 1,000 °C thermal cycling test was conducted meanwhile for comparison. Each thermal

cycle consisted of a 35 min remaining in furnace and then a 10 min immersion in room temperature flowing water.

### Isothermal exposure

The isothermal exposure test was conducted to annihilate the role of cyclic stress in the development of failure. In consideration of the very similar failure morphology at both temperatures (800 and 1000 °C) which will be discussed later in detail, two samples were kept at 1,000 °C instead of 800 °C for 5 and 30 h, respectively, for the sake of getting unambiguous experimental results. Samples were cooled down slowly within the furnace at  $\sim 2.4$  °C/min after exposure to reduce thermal stress to minimum.

### Characterization

The macroscopic photos were taken by a digital camera with an optical lens. The microstructures of TBC before and after deposition were mainly investigated by a Philips FEI SIRION 200 field emission scanning electronic microscope (FESEM). Some metallographs were taken by a JEOL JXA-8100 electron probe microanalyzer (EPMA) before samples had been etched. The distribution of chemical composition was investigated by an attached energy dispersive spectrum (EDS). The microhardness was measured by means of Vickers indentation (HX-1000 microhardness tester) at a loading of 50 g for 15 s.

## Experimental results

### Thermal cycling induced phenomena

As shown in Fig. 2a, only some vaguely cracks can be observed on the top surface after thermally cycled at 800 °C for 320 times. The sample is protected well by TBC which is free of any other failure morphologies such as spalling and buckling. However, it can be seen from

**Fig. 1** Cross-section of as-deposited sample and its schematic illustration

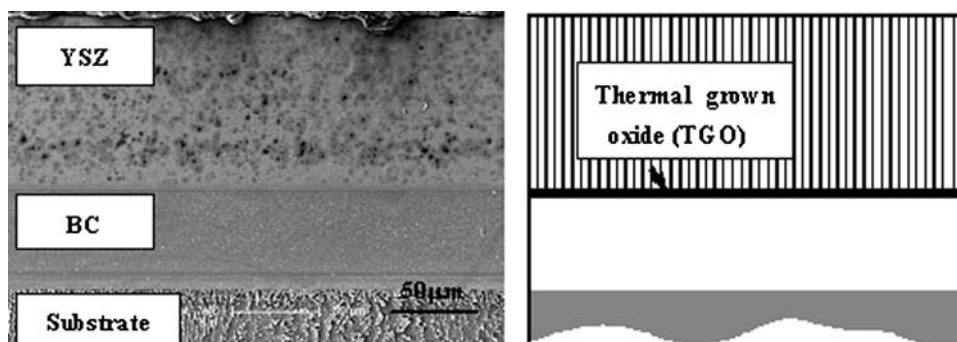


**Fig. 2** Macroscopic top surface morphology thermally cycled for 320 times: (a) at 800 °C and (b) at 1,000 °C

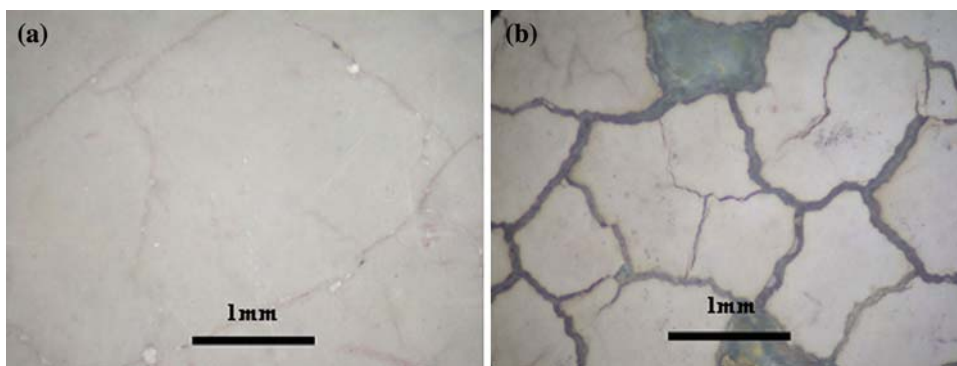


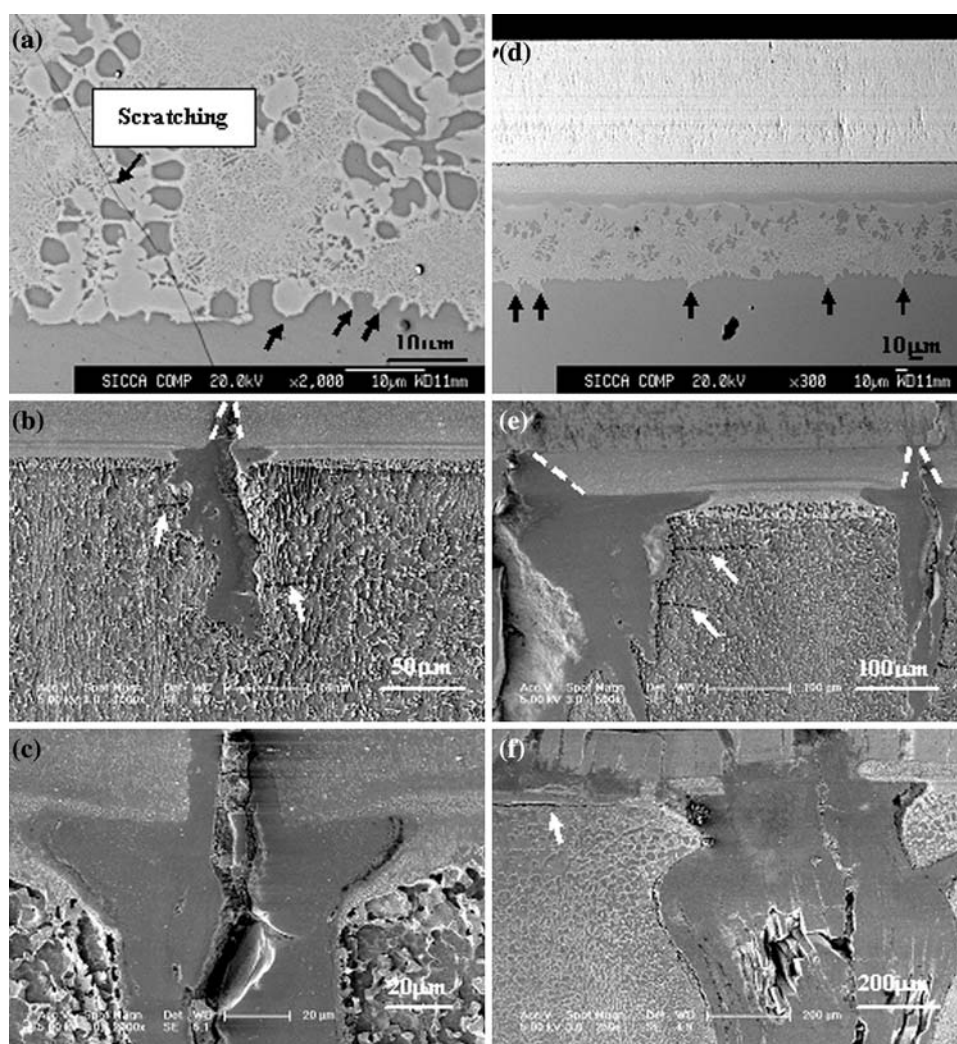
Fig. 2b that the thermal cycling at 1,000 °C results in severe cracking and spalling of the TBC. The faint yellow TiO<sub>2</sub> is observed in revealed substrate, along with a little portion of dark thermally grown oxide (TGO).

Figure 3 shows the microstructure developed after thermal cycling at 800 and 1,000 °C. In Fig. 3a, an obvious interlayer with the bright contrast in EPMA photo is arisen near the as-deposited BC/substrate interface after

thermally cycled for 10 times at 800 °C. EDS shows it is the product of interdiffusion between the BC and the substrate, and is rich in Ti, Ni, and Co. Figure 3d shows the similar diffusion pattern for 1,000 °C, with some more obvious protrusions (black arrows) immersed into the substrate.

After ~220 times thermal cycling at 800 °C, the wedge-like microcracks are developed throughout the BC with the

**Fig. 3** Microstructure development with the thermal cycling: (a) ~10 times, (b) ~220 times, and (c) 320 times at 800 °C; (d) ~10 times, (e) ~180 times, and (f) 320 times at 1,000 °C



length of  $\sim 100$  microns protruded into the substrate, as shown in Fig. 3b. One feature of these cracks is the branches formed near the as-deposited BC/substrate interface, which implies a separation of the BC from the substrate there. Another feature is the pyramid-like profile of the crack segment within BC (marked in dotted line), which indicates that the BC suffers an in-plane tensile stress from the substrate or an out-of-plane compressive stress from the ceramic, or both of them. However, the EB-PVD ceramic coating is “strain tolerant”, a relatively small amount of the tensile stress from the BC can separate the EB-PVD columnar grains of the ceramic coating. As a counterpart, the compressive stress from the ceramic is relatively small and can be negligible. Therefore, we believe this feature is mainly formed by the in-plane tensile stress from the substrate, which we will elaborate later. Then, the third feature is the fine horizontal cracks (white arrows in Fig. 3b and e) parallel to the branches, they are originated from the main body of cracks. The absence of oxide inside them suggests the presence of vertical tensile stress during cooling. Fig. 3e shows the microstructure after thermally cycled for 180 times at 1,000 °C. It can be seen that all above features are appeared and more obvious in 1,000 °C.

Table 1 shows the elements' composition in cracks shown in Fig. 3b and e, respectively. It is found that the amount of them is very approximate each other in similar domains, which, in the company of above similar failure morphology, indicates that the failure mechanisms at both temperatures are totally similar each other.

When the thermal cycling goes on, the final failure is happened after thermally cycled for 320 times at 800 °C, featured with the accumulation of oxidation products in crack, as shown in Fig. 3c. More severe failure phenomena are observed at 1,000 °C, as shown in Fig. 3f: (1) the TBC buckles upwards; (2) horizontal separation (white arrow) of the BC from the substrate is found near the as-deposited BC/substrate interface; (3) caves are observed in the crack, indicative of the volume changing of the crack during the thermal cycling.

#### Isothermal exposure induced phenomena

The macroscopic photos (in Fig. 4) show that the long-time exposure (30 h) completely failed the sample. With the

arising of the  $\text{TiO}_2$  between the BC and the substrate, the locally rumpled TBC can be easily peeled off from the sample. There are two types of local rumpling of the TBC: one is filled with the ridge-like substrate metal, and the other is filled with nothing but an empty volume, as optically and schematically shown in Fig. 4a and b, respectively. It is inferred that it is the TBC itself that initiates these rumpling, because the second type of rumpling is formed without any support of the substrate. So, the ridge-like morphology of the substrate is only the result of the rumpling of the TBC.

Figure 5 is the cross-section of oxidized substrate without the attachment of the TBC after the isothermal exposure. A crack is found within the protrusion of the diffusion interlayer, which is believed to be formed during the cooling period because of the absence of oxide inside. Furthermore, since the cooldown is very slow, the influence from the cyclic stress can be limited into the minimum, if there is still a crack formed in the diffusion protrusion, this place must be the weakest place during the service.

The cross-section of spalled TBC after 30 h isothermal exposure is shown in Fig. 6. Two types of cracks of the BC can be identified. One is shown in (a), where the BC cracks from the ceramic coating side towards the substrate side, leaving a part of the upwards buckled BC clamped in the ceramic coating. It also should be noted that the ceramic coating and BC here show an upwards buckling, which implies that the TBC buckles upward towards the ceramic side during the exposure. Such a deformation results in an out-of-plane tensile stress in the BC, which cracks the BC firstly at the ceramic side. The other type is shown in (b), where the BC cracks from the substrate side towards the ceramic coating side. This type of the crack suggests the presence of the in-plane tensile stress from the substrate during the exposure, which we find in previous thermal cycling tests.

The diffusion happened between the BC and the substrate after isothermally exposed at 1,000 °C for 2 h is shown with the distribution of chemical elements along a line passing through the TGO, BC, diffusion zone, and the substrate (Fig. 7). As can be seen, it is very violent so that the as-deposited BC/substrate interface is blurred only 2 h later. During the diffusion, a dark band appears in the BC near the as-deposited BC/substrate interface, with the width of about 10 microns because of the accumulation of Cr. Al

**Table 1** The analytical composition (at.%) of different part of cracks shown in Fig. 3b and e

	Main body			Within branches and pyramid-like part			
	Ti	O	Al	Ti	O	Al	Co, Cr, Ni
Fig. 3b	29	67	<4	29	63	<2	<5
Fig. 3e	27	71	<4	27	65	<2	<7

**Fig. 4** Revealed substrates and spalled TBCs after isothermal exposure for 30 h at 1,000 °C, as well as the schematically illustrations of two kinds of local rumpling of TBC

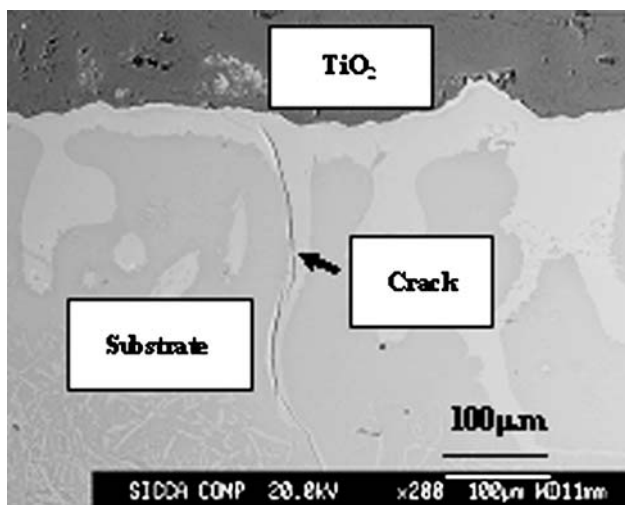
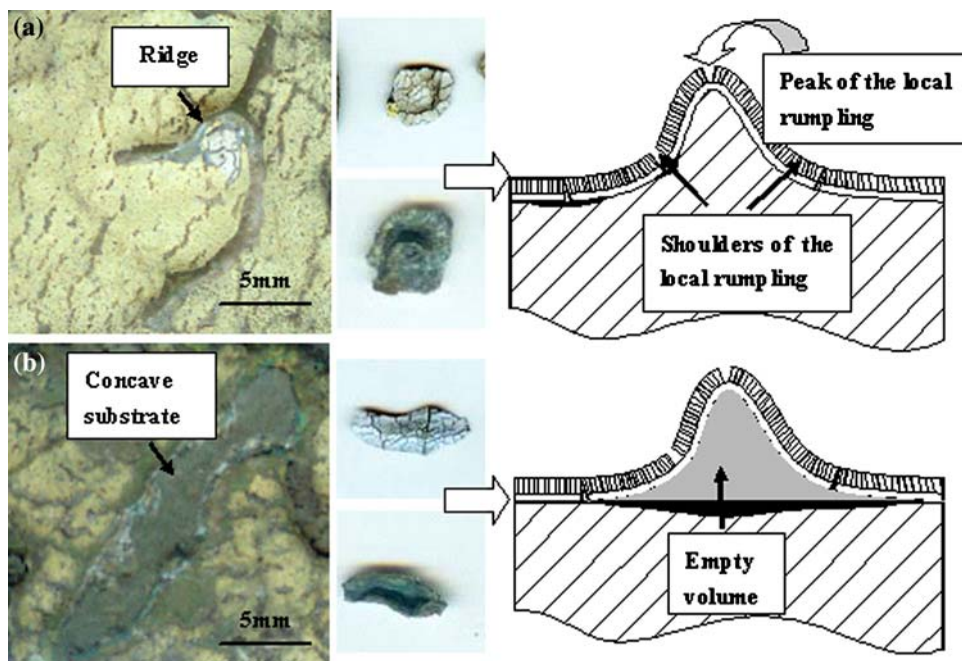
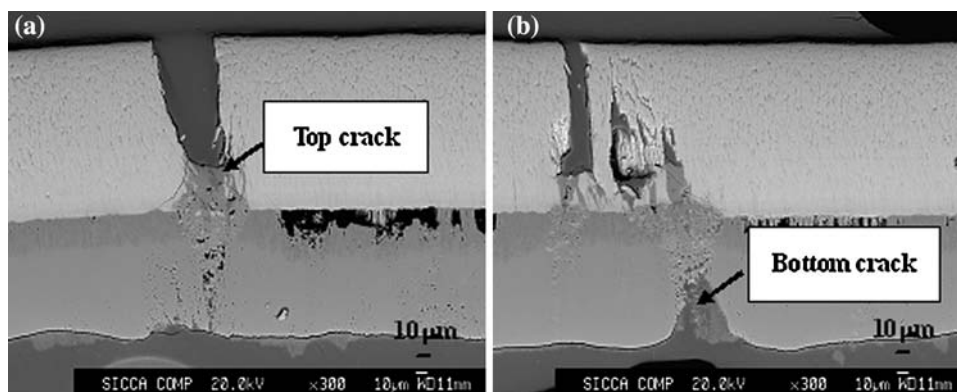


**Fig. 5** Microstructure after isothermally exposed at 1,000 °C for 30 h

diffuses to the BC/8YSZ interface to initiate the TGO. The bright diffusion interlayer is the most remarkable here, produced by the diffusion of Ni, Co to the Ti-based substrate right beside the original BC/substrate interface. EDS shows that islands with dark contrast surrounded by diffusion zone are to-be-diffused substrate, and crystal grains can be clearly recognized beside every protrusion. So the diffusion is preferentially occurred at the grain boundary of the substrate.

The diffusion affects the mechanical properties, which is reflected by the microhardness at room temperature, as shown in Fig. 8. It can be seen that the diffusion interlayer has remarkable and discrete hardness after the thermal cycling. The elevation of the microhardness can be contributed to the new diffusion products [12], and the inhomogeneity may be the result of the preferential diffusion at grain boundary. The elevation of the microhardness in the substrate is kept several hundreds of microns depth

**Fig. 6** Two different cracking morphologies in spalled TBC after isothermally exposed at 1,000 °C for 30 h



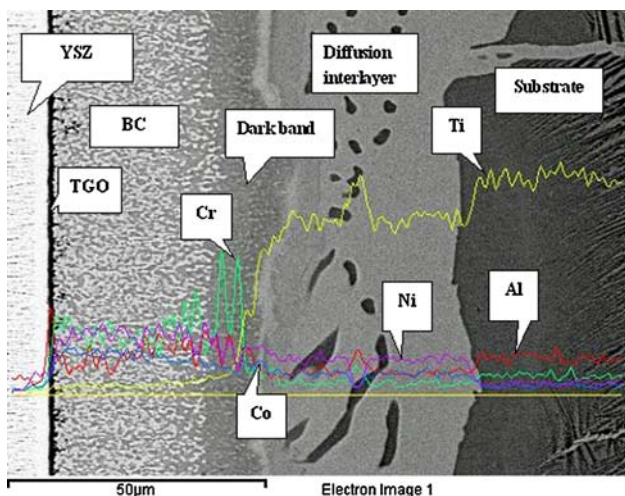


**Fig. 7** Electron microprobe scans for Ti, Al, Ni, Co, and Cr over cross-section through the whole TGO, BC, diffused zone, and substrate after 2 h isothermal exposure

from the as-deposited BC/substrate interface, forming a deep, hard diffusion-affected zone, which will unavoidably initiate the stress concentration in TBC system. The microhardness measured at the loading of 100 and 200 g show a similar tendency of the microhardness distribution of the TBC system, even though the ceramic coating is cracked.

**Discussion**

Studies for the failure mechanism of conventional duplex TBC on Ni-based alloys have been reported since the late of 1990s [13–15]. According to the computing to the residual stress in an EB-PVD TBC system [16], for which the elastic-plastic finite element models were used, the

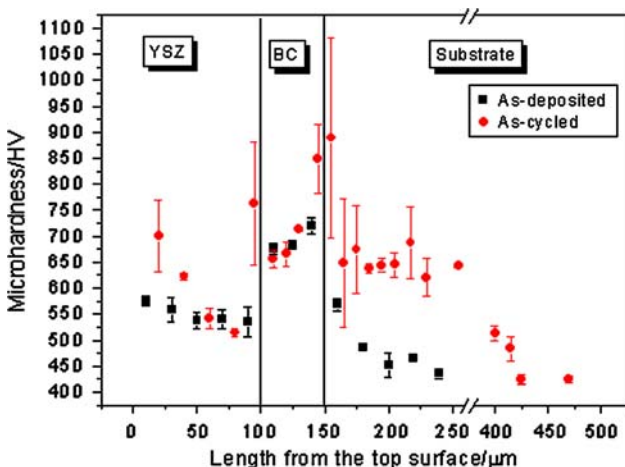


**Fig. 8** Distribution of microhardness before and after thermal cycling

mismatch of coefficient of thermal expansion (CTE) between bonded layers was believed to play an essential role to the final failure of coating system. In subsequent experimental observations, it was verified that at the planar interface, the stress field in the vicinity of the BC/TGO interface is dominated by high in-plane compressive stress in the TGO at the room temperature. However, the presence of the ridges of BC radically modifies the localized stress field and provides out-of-plane tensile stress at the peak of the ridge and in-plane tensile stress at the shoulders of the ridge at room temperature and at the ridge top at elevated temperature [14].

The experimental observations in this study show it is the vicinity of BC/substrate interface that the cracking originates from. The TGO can be ignored in current analysis because there is no evidence shows that the cracking is related with it, which may be ascribed to the prematurely cracking of BC before the TGO has been thickened enough to fail. Besides, the volume of TGO is totally not the same order as that of the BC to initiate such a large-scale failure. Meanwhile, the typical columnar grain microstructure of the 8YSZ ceramic layer can also be ignored in this discussion because of its well-known “strain tolerance”. But current failure can also be interpreted by the mismatch of CTE and the consequential tensile stress. The CTEs of the BC and the substrate are schematically illustrated in Fig. 9 [17].

At first cooldown right after deposition, because it contracts faster than substrate, the BC suffers residual in-plane tensile stress from the substrate. This may not be able to crack the BC at once, but the long-term creeping will at least cause the plastic strain in BC.

When heated to high-temperature, the BC expands faster than the substrate and the tensile stress in the BC is

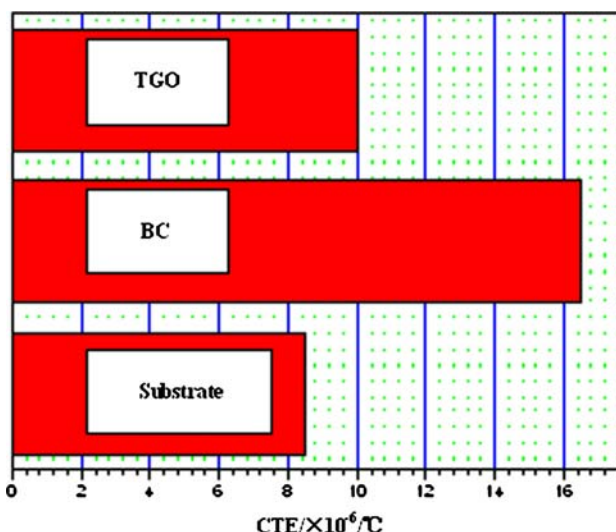


**Fig. 9** Schematic illustration of CTEs of the layered TGO, BC, and substrate of sample

relieved. However, because of the accumulation of the plastic strain and the bigger CTE than the substrate, the expanding of BC exceeds that of the substrate, as a result, the compressive stress is arisen in the BC. Been softened by high-temperature, the BC encounters the destabilizing under such a compressive stress, which upwards rumples the BC in spite of the slight resistance from the strain-tolerant 8YSZ ceramic layer. The rumpling here is more macroscopic in size than which shown in literature [18] and prefers to be formed only locally on the top surface of the sample, which may be due to the far greater order of magnitude of residual stress here. The rumpling of the BC is so considerable that the 8YSZ is permanently cracked by the entering of the top of rumpled BC to form a gap. In addition, because of the mighty metallurgical bonding between the BC and the substrate attributed to the EB-PVD technology, the upwards rumpled BC pulls a part of substrate up, causing the ridge-like deforming of the substrate, as shown in Fig. 4a. But with the presence of the diffusion interlayer, such a bonding strength is weakened, which results in the debonding in the diffusion interlayer prior to the deforming of the substrate, so nothing but an empty volume is formed by the closing of the undeformed substrate and the upwards rumpled BC, as shown in Fig. 4b. However, no matter with or without the filling of the substrate, the upward rumpling of the BC change its stress field. Out-of-plane and in-plane tensile stresses are generated at the peak and at the shoulders of the rumpled BC, respectively. The cracks at the top and at the shoulders of the rumpled BC are formed. Thus the out-of-plane and the in-plane cracking are found simultaneously in the BC, as evidenced in Fig. 6a and b. Since the metal is soft at high-temperature, these tensile stresses may not crack the BC at once, so the substrate may be kept from the oxidation, as evidenced by the ridge top shown in Fig. 4a, but the permanent plastic deformation at the peak and shoulder of the rumpled BC is formed. All of this process is described schematically in Fig. 10a.

When cooled down, the contraction of the BC has to be confronted with the ridge of the substrate, which results in the tensile stress again in the BC. Since the metal is not soft any more in cooldown, the resistance from the ridge is great enough to crack the BC from the preexisted origination of cracks to form wider cracks along the path of the ridge, as shown in spalled TBC in Fig. 4a. At the same time, the great in-plane tensile stress forms the pyramid-like cracks in the planar BC, as shown in Fig. 3b and e. Of those upwards rumpled BC without the filling of substrate, the BC contracts back into the vicinity of previous position with the permanent plastic deformation. Its cyclic alteration of the position will crack the TBC at last, but the absence of the ridge makes the cracking milder than that of the pervious, evidenced in spalled TBC in Fig. 4b. Since

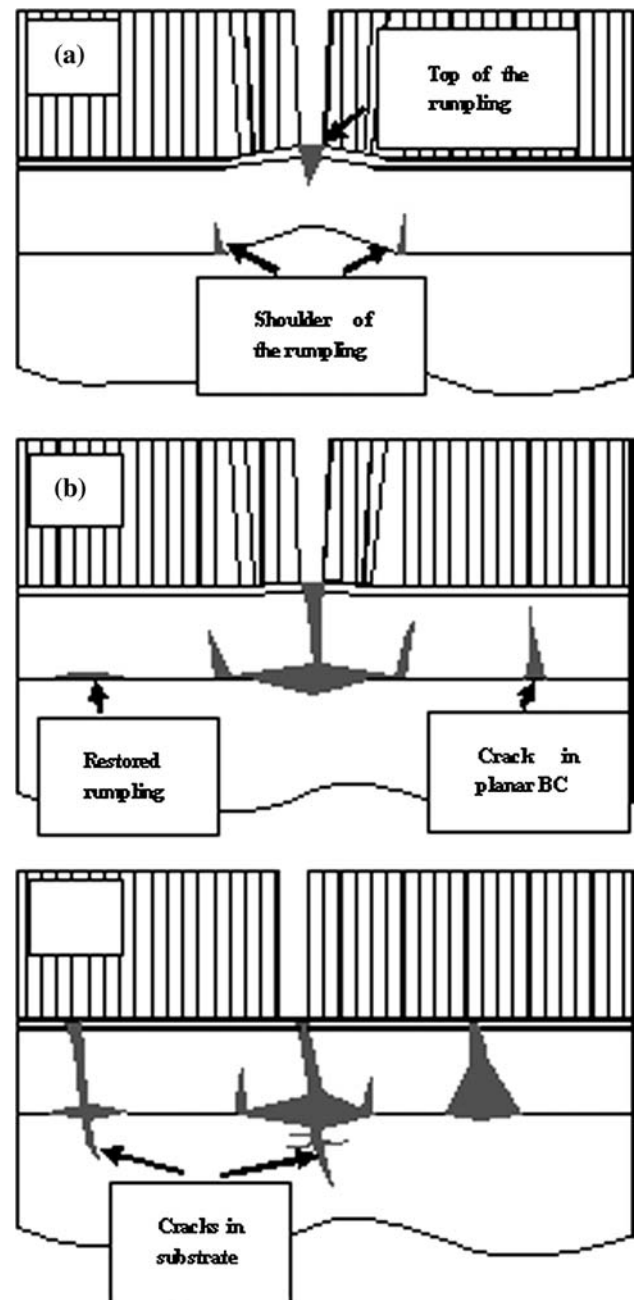


Fig. 10 Schematic illustration of the failure development

the debonding of the BC from the substrate, the characteristic branches are formed, as shown in Fig. 3b, c and e, f. However, during the same period of cooldown, the near surface of the substrate is in compressive status under the reactive force from the BC, which pushes the oxidation products up into the BC and 8YSZ ceramic layers. This can be inferred by the empty volume in the cracks shown in Fig. 3c and f. This process is illustrated in Fig. 10b.

With the development of the thermal cycling, the oxide inclusions pushed into the cracks enlarge the BC little by little. This finally turn the compressive stress in the near

surface of the substrate into the tensile stress at cooling period, initiating the cracks along the diffused grain boundaries, as illustrated in Fig. 10c. Furthermore, the oxide inclusions in the branches of crack cause the vertical tensile stress, which results in the fine cracks parallel to the branches shown in Fig. 3b and e. Thus, the final cracking morphology has been formed.

## Conclusion

The conventional duplex 8YSZ/NiCoCrAlY TBC was deposited on the near- $\alpha$  Ti-based alloy by EB-PVD method. The experimental observations to the development of failure show that:

1. The conventional duplex 8YSZ/NiCoCrAlY TBC can protect the Ti-based alloy substrate well in high-temperature for a relative short time. Its lifetime is less than 320 times of 0.5-h thermal cycling test at 800 °C. The 1,000 °C thermal cycling test will fail the coated sample sooner.
2. The diffusion of NiCoCrAlY BC to Ti-based substrate is violent, forming a hard diffusion interlayer near as-deposited BC/substrate interface, which supplies a weakest places for the debonding of the BC from the substrate and origination and propagation of the cracks.
3. With the current CTEs of the BC and the substrate, the BC will be upwards rumpled during the high-temperature exposure, which results in the cracking by the in-plane tensile stress at the shoulder and the out-of-plane tensile stress at the peak of the rumpled BC. Such a deforming of the BC pulls a part of the substrate up to form ridges, which blocks the contracting of the BC during the following cooldown to aggravate the cracking and form new cracks. Furthermore, the oxidation products of the substrate pushed into the

BC and the 8YSZ initiate the cracking of the substrate at the weakest diffused zone of the substrate.

**Acknowledgements** This research is sponsored by the Scientific Research Fund of Youth Teacher in Shanghai Jiaotong University. The authors also acknowledge Zhengzhong Yao and Jianji Feng etc. of Beijing Aeronautical Manufacturing Technology Research Institute for materials preparations.

## References

1. Leyens C, Peters M, Kaysser WA (1997) High temperature corrosion and protection of materials 4, Pts 1 and 2. Transtec Publications Ltd, Zurich-Uetikon, p 769
2. Pototzky P, Maier HJ, Christ HJ (1998) Metall Mater Trans A-Phys Metall Mater Sci 29:2995
3. Cui WF, Luo GZ, Zhou LA, Hong QA (1998) Rare Metal Mat Eng 27:348
4. Leyens C, van Liere JW, Peters M, Kaysser WA (1998) Surf Coat Tech 109:30
5. Mabuchi H, Tsuda H, Kawakami T, Nakamatsu S, Matsui T, Morii K (1999) Scr Mater 41:511
6. Gnedenkov SV, Gordienko PS, Sinebrukhov SL, Khrisanphova OA, Skorobogatova TM (2000) Corrosion 56:24
7. Gurrappa I (2003) Oxid Met 59:321
8. Zhou CG, Cai F, Xu HB, Gong SK (2004) Mater Sci Eng A-Struct Mater Prop Microstruct Process 386:362
9. Hardt S, Maier HJ, Christ HJ (1999) Int J Fatigue 21:779
10. Dimiduk DM (1999) Mater Sci Eng A-Struct Mater Prop Microstruct Process 263:281
11. Padture NP, Gell M, Jordan EH (2002) Science 296:280
12. Liu HP, Hao SS, Wang XH, Feng ZX (1998) Scripta Mater 39:1443
13. Clarke DR, Christensen RJ, Tolpygo V (1997) Surf Coat Technol 94–95:89
14. Gell M, Vaidyanathan K, Barber B, Cheng J, Jordan E (1999) Metall Mater Trans A-Phys Metall Mater Sci 30:427
15. Evans AG, Mumm DR, Hutchinson JW, Meier GH, Pettit FS (2001) Prog Mater Sci 46:505
16. Cheng J, Jordan EH, Barber B, Gell M (1998) Acta Mater 46:5839
17. Mumm DR, Evans AG (2000) Acta Mater 48:1815
18. Clarke DR, Levi CG (2003) Ann Rev Mater Res 33:383